International Journal of Civil Engineering

Structural Engineering

Experimental and numerical study of strengthened single storey brick building under torsional moment

A. A. Tasnimi[1,*], **M. A. Rezazadeh**[2]

Received: December 2010, Revised: December 2011, Accepted: January 2012

Abstract

The torsional capacity of unreinforced masonry brick buildings is generally inadequate to provide a stable seismic behavior. The torsional strength is believed to be the most important parameter in earthquake resistance of masonry buildings and the shear stresses induced in the bed joints of such building's walls is an important key for design purposes. Brick buildings strengthened with wire-mesh reinforced concrete overlay are used extensively for building rehabilitation in Iran. Their quick and simple applications as well as good appearance are the main reasons for the widespread use of such strengthening technique. However, little attention has been paid to torsional strengthening in terms of both experimental and numerical approach. This paper reports the response and behavior of two single-story brick masonry buildings having a rigid two-way RC floor diaphragm. Both specimens were tested under monotonic torsional moment.Numerical work was carried out using non-linear finite element modeling. Good agreement in terms of torque–twist behavior, and crack patterns was achieved. The unique failure modes of the specimens were modeled correctly as well. The results demonstrate the effectiveness of reinforced concrete overlay in enhancing the torsional response of strengthened building. Having evaluated the verification of modeling, an unreinforced brick building with wall-to-wall vulnerable connections was modeled so that the effect of these connections on torsional performance of brick building could be studied. Then this building was strengthened with reinforced concrete overlay and the effect of strengthening on torsional performance of brick buildings with vulnerable connections was predicted numerically.

Keywords: Brick building, Numerical micro-modeling, Strengthening, Torsional behavior, Vulnerable connection

1. Introduction

Most of the existing unreinforced masonry brick buildings in Iran are vulnerable. The lack of seismic strength and ductility of such buildings is a major problem concerning the economical loss and heavy casualties in the event of a severe earthquake. Due to the existence of numerous residential and non-residential unreinforced masonry brick buildings in the country, reconstruction is not the overall and possible solution for most of the cases. On the other hand, the need for strengthening unreinforced masonry brick buildings has been recognized for a long time by investigators as one of the effective solutions to survive the people. However, there are instances where the available lateral resistances of such building's walls are inadequate. In that perspective, various possible retrofit strategies might be used to preserve the desirable in-plane and out of plane strength while increasing the lateral strength and ductility. In past numerous experimental and numerical investigations have been conducted to find out the seismic behavior of several strengthening techniques such as shotcrete, grout injection, FRP sheets, external reinforcement, and central resistant coreused for unreinforced masonry walls subjected to in-plane and out of plane loading[1-10].

It is also reported that the use of FRP compositesincreases the strength and changes the failure modes of masonry walls. However, there are problems such asanchorage, limiting energy dissipation, brittle failure mode, time spending and expenses [3]. Extensive researches showed that the use of shotcrete or FRP would be more suitable for retrofitting of masonry buildings [4]. For transferring the shear stress across shotcrete-masonry interface, use of shear dowels (6-13 mm diameter @ 25-120 mm) are suggested. Others believe the steel ratio would control cracking, and for better bonding of brick-shotcrete, and agent like epoxy should be sprayed on the brick wall surface. Also, they proposed minimum thickness of 60 mm for strengthening layer [7-10].

* *Corresponding Author: tasnimi@modares.ac.ir*
1 Professor in Structural Eng., Faculty of Civil and Environmental Eng., TarbiatModares University, Tehran, Iran
2 MSc. Student, Faculty of civil and Environmental Eng., TarbiatModaresUniversity,Tehran, Iran

[Downloaded from ijce.iust.ac.ir on 2024-08-14]

Among the various retrofitting strategy, the simplest methods of strengthening is the use of concrete overlay reinforced with steel mesh. The concrete overlay is composed of sand-cement mortar and the steel reinforcement is wire mesh with low diameter (4-10 mm) bars. This method is simple, easy and adequately quick compare to other methods. An additional benefit of the reinforced concrete overlay would be the enhanced out-of-plane wall resistance, which is beyond the scope of this study. Moreover, previous experimental researches on strengthening brick walls with reinforced concrete overlayhave shown that this method improves lateral strength and ductility [4].Nevertheless, there are relatively few experimental results available in the literature devoted to the study of unreinforced and strengthened brick buildings under torsional moment.

In present paper, the results of a combined experimental and numerical study on two full-scale one-story brick buildings under torsional moment are presented. One of the buildings is unreinforced brick buildings as a control specimen and the other is strengthened unreinforced brick building. Experimental tests have been conducted on both buildings having a rigid two-way reinforced concrete slab, and have been loaded until failure by means of two-concentrated horizontal force, after the application of vertical load equal to 80kN.Numericalfinite element analysis have been conducted on both buildings in order to have a better insight into the structural behavior of the buildings experimentally analyzed. This modeling was of a micro-modeling type in which separate elements were defined for each masonry units, mortar and surface contacts between bricks and mortar. Adetailed comparison between experimental evidences and numerical results is finally presented. Good agreement between experimental data and numerical predictions is found, meaning that the combined numerical/experimental analysis conducted may represent a valuable reference for engineers involved in the evaluation of the torsional capacity of strengthened brick buildings.

2. Experimental Program

2.1. Material properties

During the construction of test specimens, quality control samples were obtained to find the mechanical characteristics of bricks, mortar, concrete, steel bar and masonry units.The bricks were of clay bricks type with nominal dimension 203x94x52 (mm). Bending and compressive strength of bricks were tested according to ASTM C-67-00[11]. Compressive and splitting tensile strength of concrete used in the roof and foundation for both of the buildings were set according to ASTM C 39/C 39M-99 and ASTM C 496-96 respectively [12& 13].

The concrete for all specimens was made from type-I Portland cement, river sand, and 16mm maximum size crushed gravel. Measured slumps ranged from 60mm to 90mm for all specimens. From the six 150 x 300mm concrete cylinders, three were tested in compression at 28 days and the remaining three used for the tensile splitting test. Also compression tests were carried out on 150 x150mm cubes. The modulus of elasticity of concrete was calculated on the basis of data obtained from cylinder compression tests.

The mortar's mix proportion (cement to sand) for walls and for the concrete overlaywere 1:5 and 1:3 respectively. Standard tests of compressive, tensile, bending and shear strength were carried out for5-course masonry prismsto determine their mechanical characteristics (ASTM C-1314-00a) [14].Table 1 summarizes the results of the tested material.

In this investigation, the average compressive strength of masonry prisms was less than the average compressive strength of the used bricks and higher than that of mortar. This is due to different material properties that cause vertical splitting of the bricks to occur prior to the crushing of the

Table 1. Material Properties

Sample type	No of samples	Test Description	(MPa)
Brick	5	Compressive strength of bricks	9.25
	5	Bending strength of bricks	5.14
Concrete slab, Foundation	6	Compressive strength of concrete cube	25.1
	6	Elastic modulus of concrete	19227.5
	3	Tensile strength of concrete	1.995
Wall's Mortar	3	Compressive strength of mortar	3.07
	3	Tensile strength of mortar	0.78
		Elastic modulus of mortar	795
concrete overlay	3	Compressive strength	30.04
Steel Bar Slab, Foundation and cover	3	Yield tensile strength of barΦ10	339.5
	3	Yield tensile strength of bar Φ6	310.1
	3	Yield tensile strength of barΦ4	318
Masonry units	5	Compressive strength of masonry unit	5.07
		Elastic modulus of masonry unit	1200
	3	Tensile strength of masonry unit (bending beam test)	0.058
	3	Tensile strength of masonry unit (diagonal pressure test)	0.65
	5	Cohesive strength of masonry unit	0.14
		Coefficient of internal friction (k)	0.53*

* This constant value has no unit

[Downloaded from ijce.iust.ac.ir on 2024-08-14]

mortar. It is stated that the higher Poisson's ratio of the mortar results in a tendency for lateral mortar tensile strains to exceed the lateral brick rupture strains (Paulay and Priestley) [15].

Therefore, the normal compression and lateral biaxial tension in the bricks reduces its crushing strength and induces a tendency for vertical splitting. Masonry prisms failure occurs after the vertical splitting strength of bricks is exceeded which is less than the compressive strength of the bricks.

As there is no ASTM testing procedure given for shear test of masonry samples, the modified triplet specimen for pure shear was used to obtain the mortar shear strength and friction coefficient (Harris and Sabnis [16]). This specimen represents the actual shear loading case of masonry walls along the mortar bed-joints. The average values of angle of friction (ϕ) and coefficient of cohesion (c) from three prism samples were obtained when they are loaded up to fracture using various constant compression forces together with increasing shear forces.

2.2. Test specimens

Two full-scale single-story brick buildings were constructed and tested under monotonic torsional moment. Geometrical characteristics of both specimens were similar and were constructed and tested in the structural engineering laboratory at the Building and Housing Research Center (BHRC). The length, height and thickness of the walls were 2020mm, 1500mm and 220mm respectively. Both buildings were monolithically connected to the foundation, which was utilized to fix down them to the laboratory's strong floor, simulating a fully fixed footing. The connection of both specimens to the strong floor was made by use of steel channels (UNP300- 2100 x 2100 mm) fixed to the strong floor by use of high strength steel bolts of 24 mm diameter. To prevent the possible sliding of reinforced concrete foundation the angles of 100 x 100 x10 mm welded to the channel as shear connecters. The foundation reinforcements were placed into the steel channels after which the concrete poured (Figure 1). All displacement measurements were carried out using linear transducers (LVDT). Figure 2

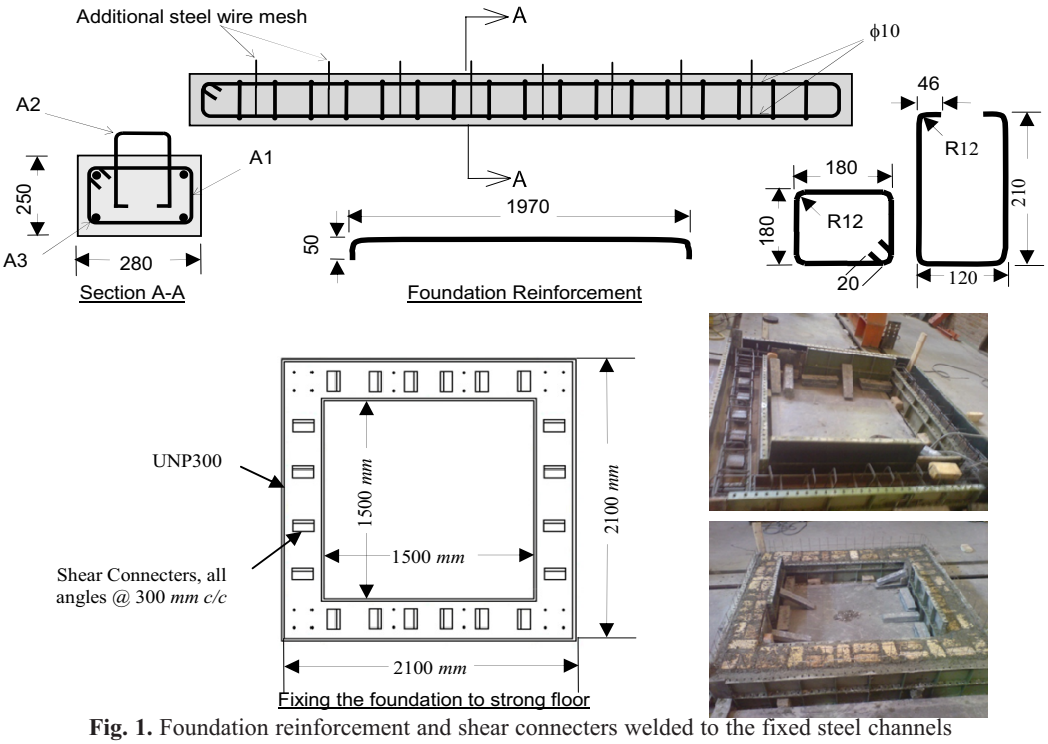

Fig. 1. Foundation reinforcement and shear connecters welded to the fixed steel channels

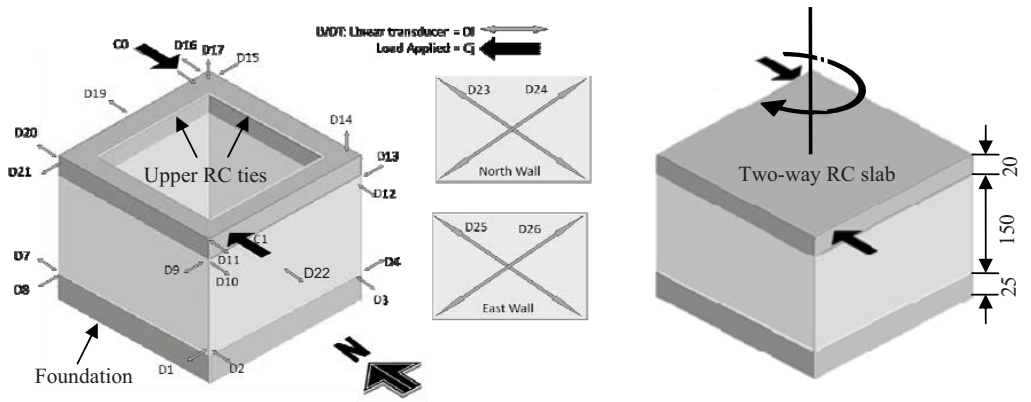

Fig. 2. Schematic representation of tested buildings with the location of LVDTs

[Downloaded from ijce.iust.ac.ir on 2024-08-14]

illustrates the location of all LVDTs and their relevant coding number. Table 2 provides the channel number of each LVDTs location to record the measured quantities.

2.3. UBB specimen

The primary specimen was an unreinforced brick building designated as UBBand considered as the control specimen. This specimen provides good information for unreinforced brick buildings under pure torsion having no effect of openings on its behavior. In addition, its results are a good measure for comparison with that of strengthened specimen. For construction of RC slab, it was not possible to use ordinary supports as there was no access inside the building and hence hanging support was employed by providing special hook type support as illustrated in figure 3. An experienced mason constructed both specimens. According to the requirements of the Iranian National Building Code-Part 8 [17], all bricks were presoaked to decrease the water absorption from the mortar joints to improve the bond strength at the brick-mortar interface. All walls had full bed and head joints. The roof of both buildings was made of two-way RC slab to equally distribute the torsional moment.

Table 2. Location of the measurement's devices on the specimens

Ref. to Fig.1	Channel No. location Specimen (Building)		Ref. to Fig.1	Channel No. location Specimen (Building)	
	SUBB	UBB		SUBB	UBB
D_1	25	27	D_{15}	11	15
D_2	18	20	D_{16}	7	7
D_3	19	21	D_{17}	27	11
D_4	20	22	D_{18}	12	16
D_5	21	23	D_{19}	17	9
D_6	22	24	D_{20}	13	17
D_7	23	25	D_{21}	14	18
D_8	24	26	D_{22}	16	8
D_9	15	19	D_{23}	4	4
D_{10}	8	12	D_{24}	5	5
D_{11}	6	6	D_{25}	3	3
D_{12}	9	13	D_{26}	2	2
D_{13}	10	14	C_0	0	0
D_{14}	26	10	C_1	1	1

2.4. SUBB specimen

The second specimen was completely similar to the control specimen and the out surface of its walls were strengthened with concrete overlay reinforced with steel mesh and designated as SUBB.The thickness of concrete overlay was 40mm. Steel mesh of ribless-bar type with diameter of4mm and spacing of 100 mm were used to reinforce this concrete overlay. This steel wire mesh was attached to the brick wall by ϕ6 anchors300 mm apart.For the purpose of integrity, it was required to provide additional steel wire mesh into the foundation before concreting. These additional wire meshes were tied to the reinforcement of the concrete overlay around the specimen.To homogenize roof and foundation with walls, an extra raw of walls constructed in such a way to be merged with the upper RC tie and with the foundation. In addition, 80mm length of reinforcement inserted into the vertical bonds of the extra raw of the walls that was extended into the upper ties. In the lower part,150 mm extra height of the steel wire mesh was connected to the upper

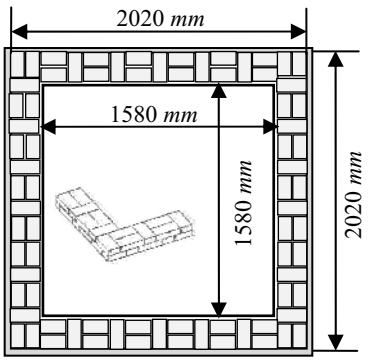

a) Integrated first raw of Brick walls

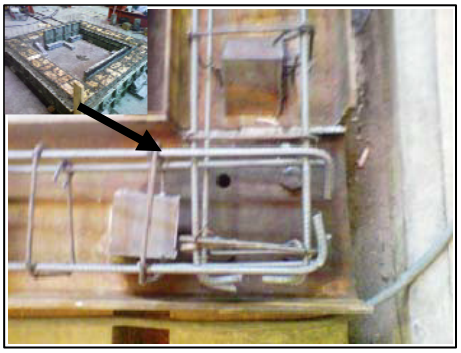

b) Construction of foundation and first raw with steel wire mesh connected to foundation

c) Reinforcing and concreting of slab and upper tie

d) Instrumented specimen ready for test

Fig. 3. Making Specimen UBB ready for test

[Downloaded from ijce.iust.ac.ir on 2024-08-14]

tie's reinforcement to have uniformity between wall and concrete overlay. Figure 4 illustrates some photos of the construction of this specimen.

2.5. Test setup and loads applied

Two different systems of gravity and horizontal monotonic loading were applied. The 8 tons subjected gravity load was equal to a double-floored brick building with the dead load and live load of 600 and 200 kg/m^2 respectively. This gravity loading was statically applied by putting lead bullion (each 18.4 kg) on the roof of the specimens. Hydraulic jacks were employed to apply two lateral concentrated loads, which measured through load cells installed behind them. An automatic data acquisition system was used to continuously read applied displacements and measured loads, displacements and strains. In the place where the horizontal loads were applied, two steel plates of 25mm thick were placed during the construction of upper tie for both specimens. To prevent the load path disposition due to torsional movement of specimens, a special devices were designed and constructed. These devices were positioned between hydraulic jacks and specimens as shown in Figure 5.

2.6. Testing procedures

All displacement measurements were carried out using linear transducers (LVDT). Figure 2 illustrates the location of all LVDTs and their relevant coding number. Table 2 provides the channel number of each LVDTs Location. The measured values of load, displacement were recorded by a computer data logger capable of measuring to sensitivity ranges of 1N, 0.001 mm respectively, with speed of about 0.08 Second per channel. After installing displacements and load cells, the specimens were ready for tests.However, after applying the gravity load, the specimens were subjected to monotonic torsional moment. Loading continued until the failure of specimens occurred.

3. Experimental Results

3.1. Specimen UBB

All specifications of this specimen were briefly discussed in previous sections. The loads applied incrementally through both hydraulic jacks and cracking started diagonally in the direction of applied torsional moment in the walls of the buildings. The first visible crackappeared at 157.9kN-m. There was no significant cracking at this stage in the roof and only hair cracks were expanded from wall to the upper tie. This is a good indication of monolithic connection between roof and brick walls. By increasingthe load,cracks widened and concentrated until the failure occurred at a torsional moment equivalent to 9.4% drop of maximum value (201kN-m) in post-peak state.The average rotational displacement around the vertical axis of the building was calculated upon the

a) Brick walls, Wire-mesh and Top tie's reinforcement

b) Concrete overlay on the steel wire mesh

c) Slab reinforcement and hanging support

d) Instrumented specimen ready for test

Fig. 4. Making Specimen SUBB ready for test

[Downloaded from ijce.iust.ac.ir on 2024-08-14]

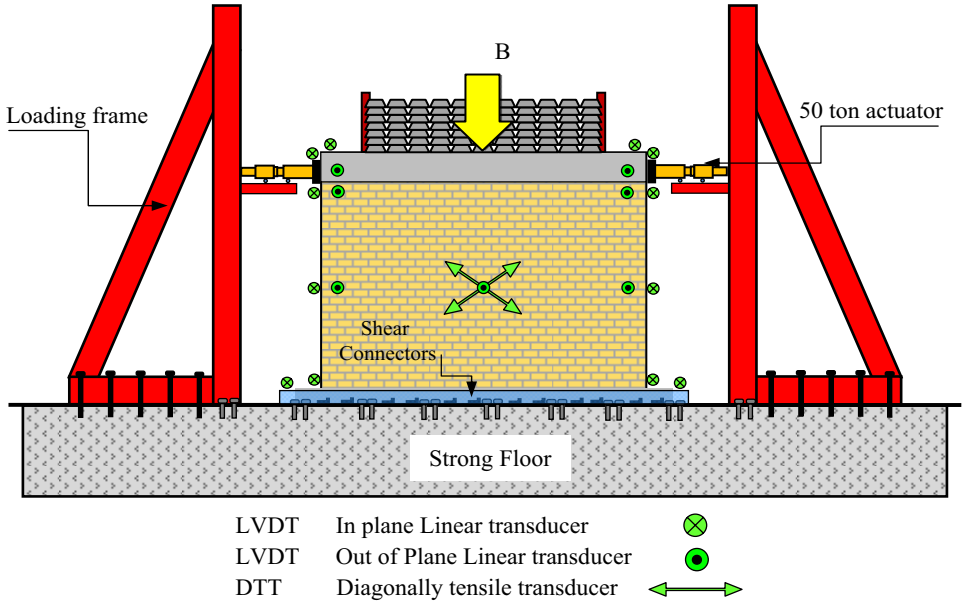

a) Schematic testing setup system

b) Application of loading system

c) Detail of Self controlled applied loading system

Fig. 5. Testing setup, instrumentation and loading system details

movement of each corner at roof level. Figures 6a-6d shows the crack pattern and Figures 6e-6i provides the behavior of the specimen in the form of torque-twist relationship with the individual states of behavior that represented by linear regression with acceptable coefficient of correlation.

3.2. Specimen SUBB

For this specimen also all the specifications were briefly discussed in previous sections. The loads applied incrementally through both hydraulic jacks and distributed diagonal cracks appeared in the direction of applied torsional moment to the walls of the building. In this specimen,due to presence of the reinforced concrete overlay in preventing stress concentration, cracks were more distributed. Minor cracks developed at east-north corner of north wall at 126.8kN-m. The first visible crack appeared at 293.6kN-m on same wall with the direction of west-north corner towards the center of wall. At load 312.1kN various cracks parallel to the diagonal crack developed. After the peak load, more distributed cracks developed and some previous cracks widened. Near failure,diagonal crack of east wall widened and on south and west walls adjacent to foundation, horizontal cracks developed and widened. After the maximum torsional moment (624.2kN-m) where the cracks widened some reinforcement broken and the test stopped not to cause any inconvenience. However, the failure mode of this specimen was a combination of diagonal and sliding cracks. Figures 7a-7d show the crack pattern and Figures 7e-7i provide the behavior of the specimen in the form of torque-twist relationship with the individual states of behavior that represented by linear regression with acceptable coefficient of correlation.

4. Theoretical Background for numerical modeling

In order to validate the experimental results, non-linear numerical analysis was carried out based on micro modeling for tested buildings. In this model, the behavior of bricks and mortar is assumed to obey the plastic-damage model and for different damage states two damage variables including tensile and compressive was employed. In summary, the elastic-plastic response of the damaged plasticity model is described in terms of the effective stress and the hardening variables. The

[Downloaded from ijce.iust.ac.ir on 2024-08-14]

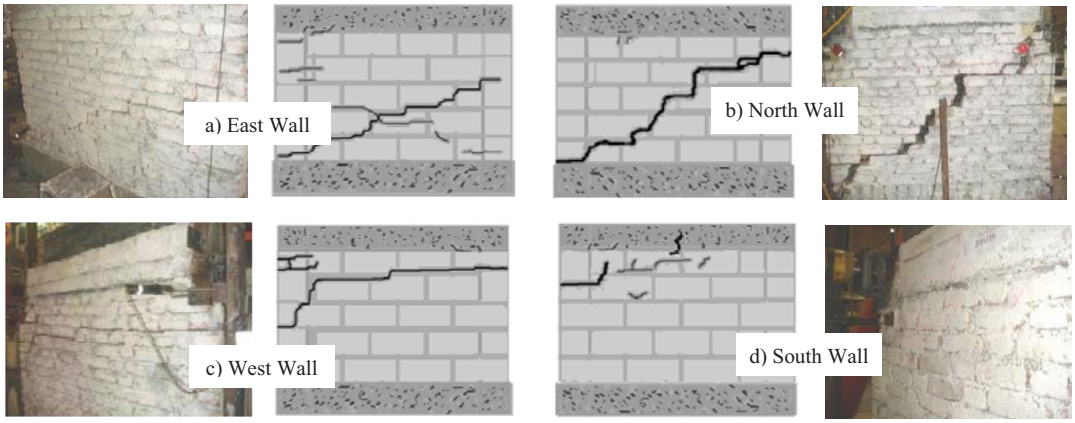

Cracking of walls during test

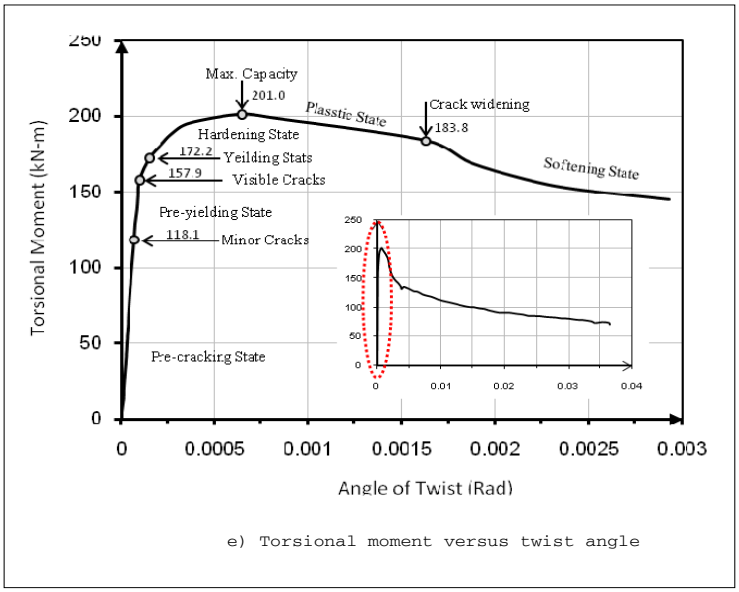

e) Torsional moment versus twist angle

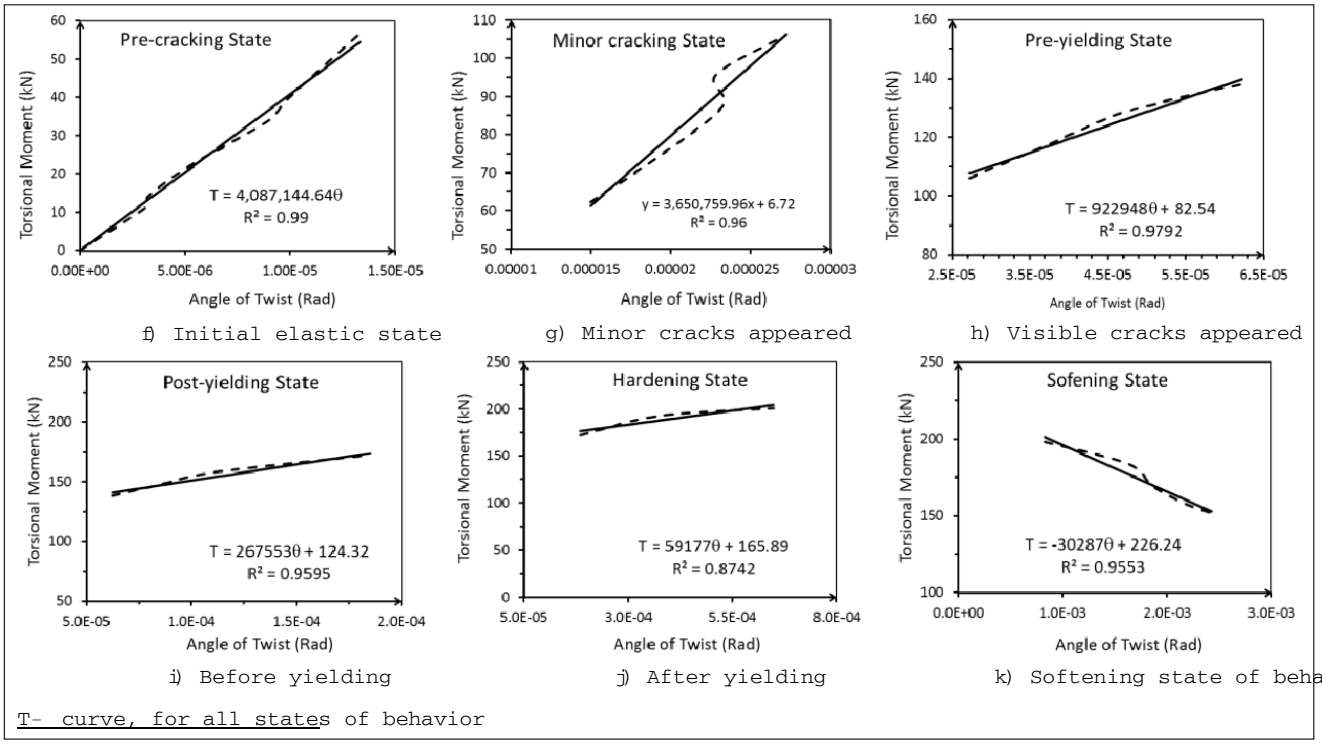

f) Initial elastic state g) Minor cracks appeared h) Visible cracks appeared

i) Before yielding j) After yielding k) Softening state of behavi

T- curve, for all states of behavior

Fig. 6. Crack pattern and torque-twist relationship, specimen UBB

[Downloaded from ijce.iust.ac.ir on 2024-08-14]

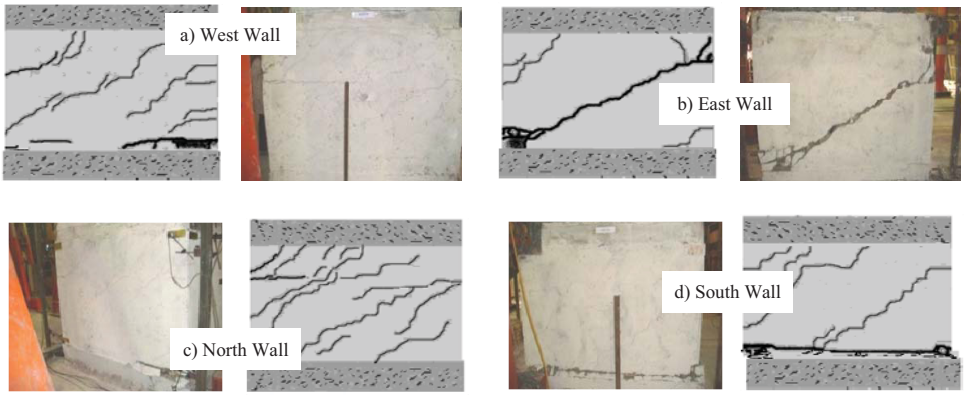

Cracking of walls during test

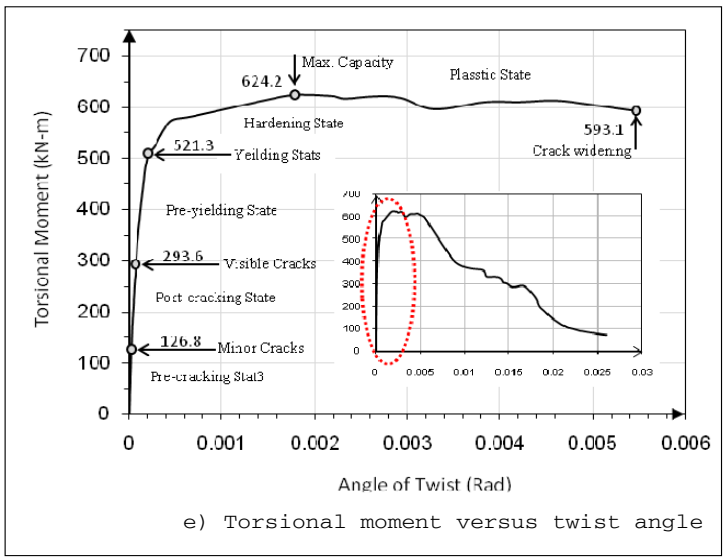

e) Torsional moment versus twist angle

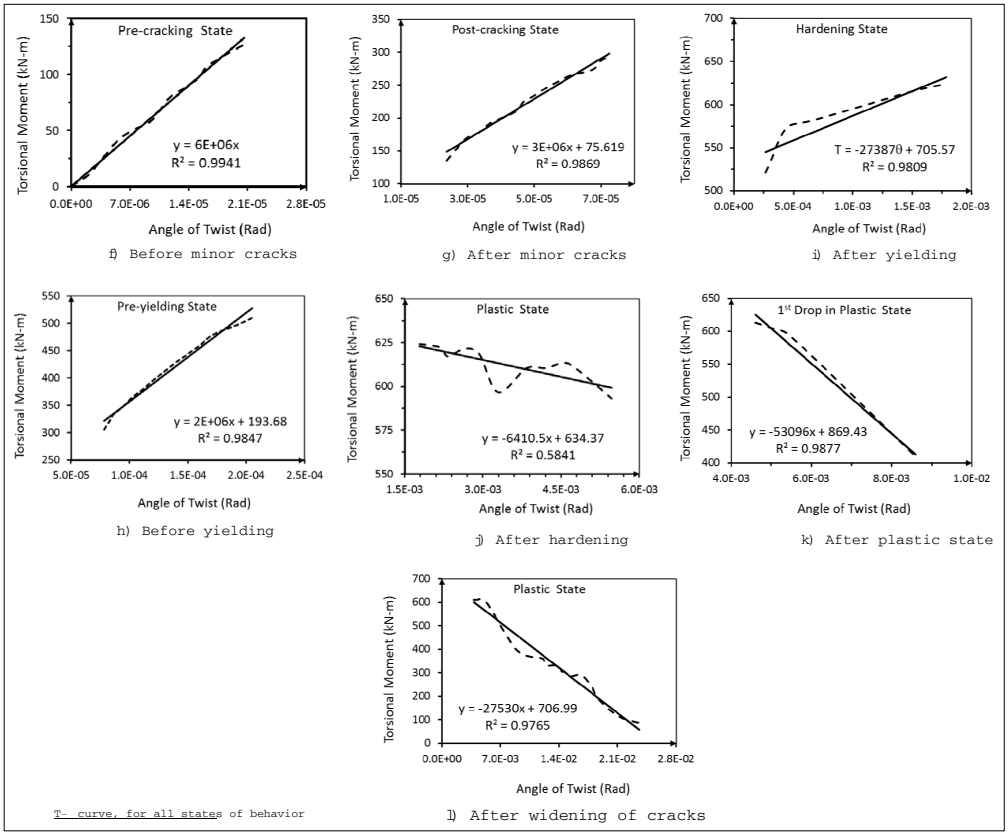

f) Before minor cracks
g) After minor cracks
i) After yielding
h) Before yielding
j) After hardening
k) After plastic state
T- curve, for all states of behavior
l) After widening of cracks

Fig. 7. Crack pattern and torque-rotation relationship, specimen SUBB

[Downloaded from ijce.iust.ac.ir on 2024-08-14]

strain tensor and strain rate are decomposed into the elastic and plastic parts. The stress-strain relations for bricks and mortar are governed by scalar damaged elasticity. Damage associated with the failure mechanisms of the masonry (cracking and crushing) results in a reduction of the elastic stiffness. Within the context of the scalar-damage theory, the stiffness degradation is isotropic and characterized by a single degradation variable. When damage occurs, however, the effective stress (resisting the external load) is more representative than the stress. It is, therefore, convenient to formulate the plasticity problem in terms of the effective stress.

Hardening variables control the evolution of the yield surface and the elastic stiffness degradation and referred to the dissipated fracture energy required to generate micro-cracks. Therefore, micro cracking and crushing in brick or mortar as quasi-brittle materials are represented by increasing values of the hardening variables. However, tensile and compressive damages are quite different in such materials and it is not possible to represent all damage states by a single parameter. Therefore, for different damage responses of brick or mortar in tension and compression, a multi-hardening or multi-softening yield function is used. The degradation of the elastic stiffness is significantly different between tension and compression and as the plastic strain increases in either case, the effect is more pronounced. The degraded response of masonry is characterized by two independent uniaxial damage variables, which are assumed functions of the equivalent plastic strains. Under uniaxial loading, cracks propagate in a direction transverse to the stress direction. The distribution and propagation of crack, therefore, causes a reduction of the available load-carrying area, which in turn leads to an increase in the effective stress. The effect is less pronounced under compressive loading since cracks run parallel to the loading direction. It is obvious that after a significant amount of crushing, the effective load-carrying area is also significantly reduced.The interface between mortar and brick is modeled using coulomb friction model, which is based on maximum shear and normal stress applied to the interface. The standard coulomb friction model assumes that two materials sustain the same shear stress and no relative motion occurs if the frictional stress is less than the critical stress, which is proportional to the contact pressure. When frictional stress reaches, the critical stress slip can occur. This shear stress limit is typically introduced in cases when the contact stress may become very large, causing the Coulomb theory to provide a critical shear stress at the interface that exceeds the yield stress in the material beneath the contact surface. In this numerical modeling, cohesive elements were completely tied to brick elements and contact behavior was employed among brick elements.

4.1. Numerical modeling

The plasticity parameters for mortar and bricks needed for non-linear analysis are obtained with this view that they approximately behave same as concrete. Therefore, the concrete plasticity damage (CDP) model, was used for bricks and tension behavior model (Traction) used for cohesive elements in combination with contact element. The value of these parameters were estimated based on excellent agreement between the test results on brick prisms carried out in reference [18] and the results of numerical analysis in this work.Table 3 provides the average value of mechanical properties of tested samples and their plasticity parameters. Figure8 illustrates the deformed shape of prisms under shear and tensile load. The published Poisson's ratio values for bricks and mortar are used from other sources and not obtained experimentally here [19-23].

Dynamic explicit method performed in this numerical analysis. In order to get the static behavior through dynamic analysis, it is necessary to increase the time of analysis, which has been optimized after several analysis carried out.However, this method is only conditionally stable, and would blow-up if the time step were not short enough. It is clear that more methods that are effectiveandavailable, but this method is the simplest procedure and by adopting a shorter time step than others can be used to obtain a satisfactory representation of the

Table 3. Characteristics of tested prism

Characteristics of brick	
Elastic modulus	E_{brick}=20000 MPa
Poison ratio	υ=0.15
Density	ρ=0.000021 N/mm^3
Characteristics of cohesive element	
Elastic	K_{nn}=222 , K_{ss}=99, K_{tt}=99N/mm^3
Density	ρ=0.0000236 N/mm^3
Damageproperties	f_n= 0.03 , f_s=0.87 , f_t=0.87MPa G_n^I= 0.012 , G_n^{II} =0.58 , G_n^{III} =0.58 Nmm/mm^3
Characteristics of contact element	
Friction Coefficient	$tan\varphi$=0.73
Normal behavior	Hard Contact

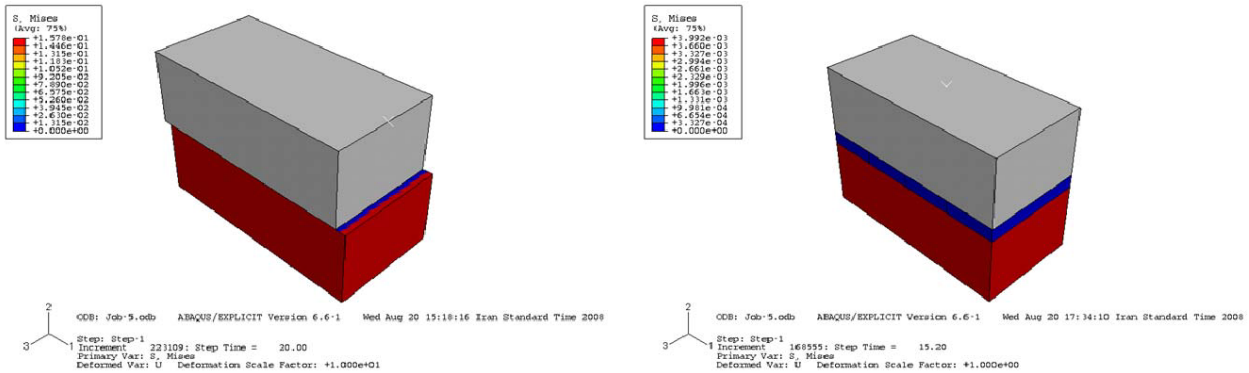

Fig. 8. Deformed shape of two bricks prism under shear and tensile load

[Downloaded from ijce.iust.ac.ir on 2024-08-14]

dynamic input and response. Using plastic-damage model and inserting material elastic and plastic properties and brick-mortar interface properties, specimens were loaded and analyzed up to failure.

4.2. Modeling of specimen UBB

The numerical analysis of tested specimen UBB with 10mm mortar thickness carried out to validate its behavior.The vertical and bed joints of the tested specimen were filled by mortar and same characteristic was considered for numerical model. The specifications of bricks, mortar, and their joints are given in Table4. The uniform distributed gravity load with the intensity of 0.019MPa applied linearly within 0 to 5 seconds. Then this load kept sustained for 10 seconds, meanwhile the lateral load also applied linearly within the 5th to 10th seconds. The loading was continued until cracking appeared and up to the threshold of collapse.

Table 4. Characteristics of materials of UBB specimen

Characteristics of brick	
Elastic modulus	E_{brick}=8080 MPa
Poison ratio	υ=0.15
Density	ρ=0.000021 N/mm^3
Characteristics of cohesive element	
Elastic	K_{nn}=240 , K_{ss}=96, K_{tt}=96 N/mm^3
Density	ρ=0.0000236
Damageproperties	f_n= 0.058 , f_s=0.14 , f_t=0.14MPa
Characteristics of contact element	
Friction Coefficient	*tan* φ=0.53
Normal behavior	Hard Contact

The numerical torque-twist curve of the specimen is drawn and compared with that of experiment with excellent agreement illustrated if Figure 10-a. The collapse mechanism with diagonal cracking through vertical and horizontal joints and bricks with toe crushing observed in the model and the experimental results. Figures 9-a and 9-b illustrate un-deformed and deformed modeling of this specimen.

4.3. Modeling of specimen SUBB

For numerical modeling of SUBB specimen, the properties of brick, mortar and contact element were same as that of specimen UBB given in Table4.The needed characteristics of concrete overlay and steel mesh are provided in Table 5. Surface element employed for modeling steel mesh that was embedded in concrete 3D element in order to model reinforced concrete elements. Since the surface of the brick walls of tested SUBB specimen was hardly rough, there was entirely complete connection between concrete overlay and the brick walls. Same connection type imposed to the numerical model by considering two contact surfaces of brick wall and concrete overlay elements. The gravity and lateral load applied to this specimen was similar to that of specimen UBB. Figures 9c and 9-d illustrate un-deformed and deformed shape of this specimen.

Experimental and numerical T-□curves for both UBB and

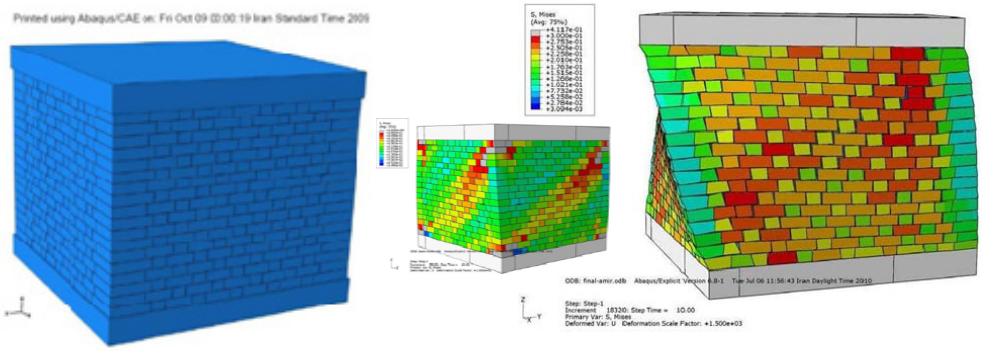

a)Unreformed Specimen, UBB b)Deformed Specimen, UBB

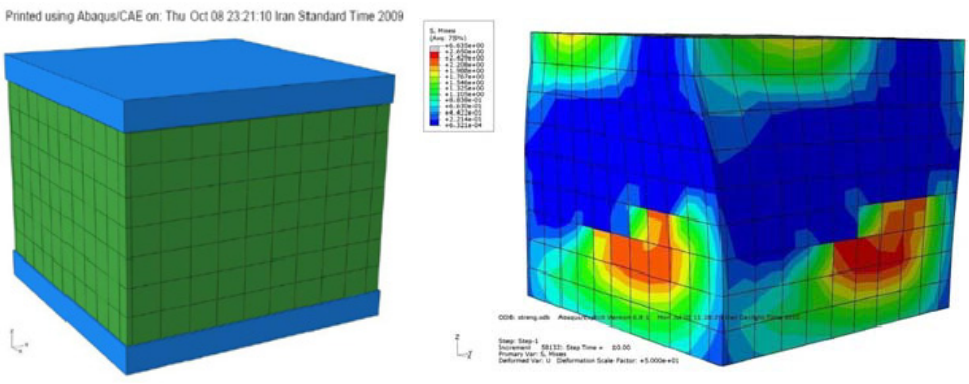

c) Unreformed Specimen, SUBB d) Deformed Specimen, SUBB

Fig. 9. Un-deformed and deformed shape of specimens UBB and SUBB

[Downloaded from ijce.iust.ac.ir on 2024-08-14]

SUBB buildings are prepared and shown in Figure 10-a and 10-b. In this, goodagreement between the numerical and experimental torque-twist relationship is illustrated.Table 6 gives the torsional moment for different states of behavior and their relevant ratios. The ratio of torsional moment of strengthened specimen to that of unstrengthened specimen for various state of behavior is 2.03, 2.76, 3.77, 3.25, 3.11 and 3.23 respectively and the ratio for elastic torsional rigidity is 1.56. These are good indication of the effect of RC overlay as a simple and rapid strengthening method to be used for masonry buildings. In the same table the above ratios of numerical models (NUBB and NSUBB) to their relevant tested specimens indicates close agreement between numerical and experimentalresults. The underestimated ratio of elastic torsional rigidity of numerical to experimental is 0.78 and 0.71 for unstrengthened and strengthened specimens respectively.

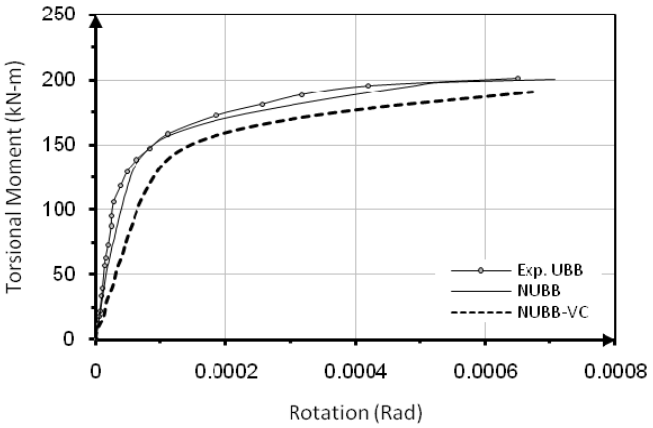

a)Specimen UBBs, T-θ curve

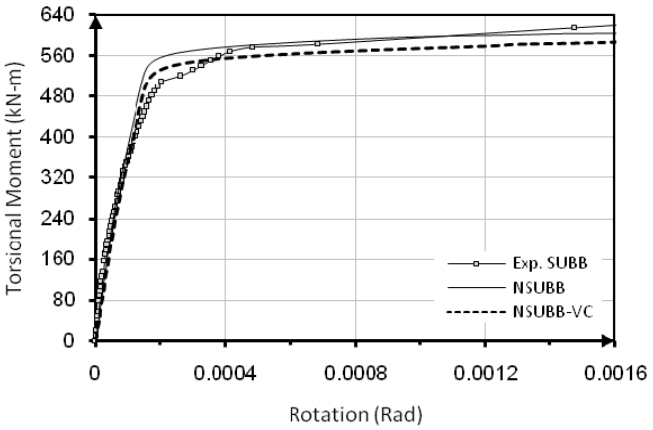

b) Specimen SUBBs,T-θ curve

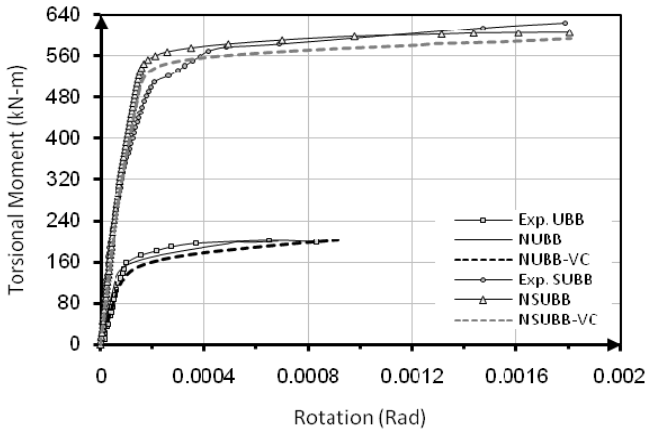

c) Comparison of Experimental and Numerical T-θ curves of all specimens

Fig. 10. Experimental and numerical T-θcurve of both buildings

4.4. Effect of wall-to-wall connections on torsional performance

According to the Iranian code of practice for earthquake resistant building design (IS-2800), the connection of wall-to-wall is not allowed except the vertical RC ties are constructed simultaneously with walls [24]. Nevertheless, most of the existing brick buildings are not constructed according to IS-2800 and are vulnerable from their wall-to-wall connections.

To investigate the effect of the strengthening method used in this paper on the wall-to-wall connection, which was one of the failure modes in some earthquakes shown in Figure 11, it was decided to model the wall-to-wall connection in numerical analysis and quantifying the strengthening effect on the torsional capacity of brick buildings.

In this regard in addition to the previous numerical analysis carried out, another two strengthened and unstrengthened numerical models made with the vulnerable wall-to-wall connections. They are designated as NSUBB-VC and NUBB-VC respectively. The vulnerable connection was assumed by considering the almost zero value for the properties of bricks (density, elastic modulus, compressive and tensile strength) and for mortar in both horizontal direction (density, elastic modulus, tensile and shear stress). It is obvious that the length of the walls of vulnerable building reduces to 1.58m. The slab of both vulnerable buildings was a two-way RC rigid diaphragm on a rigid base. Therefore, no interaction between these walls would be experienced. Figure12 illustrates the schematic comparison between the two wall-to-wall connections assumed for numerical analysis.

The result of this numerical analysis in the form of T-□ curve is compared with that of experimental and previous numerical models to illustrate the strengthening effect on torsional

Table 5. Characteristics of reinforced concrete overly material of SUBB specimen

Characteristics of concrete overlay	
Elastic modulus	E=25000 MPa
Poison ratio	υ=0.2
Density	ρ=0.000024 N/mm^3
Dilation Angle	25
Eccentricity	0.1
Concrete Damage	f_{b0}/f_{bc}=1.16
Plasticity	K=0.67
Viscosity Parameter	0
Characteristics of steel mesh	
Elastic modulus	E=190000 MPa
Poison ratio	υ=0.3
Density	ρ=0.000077 N/mm^3
Yield Stress	f_y=300 MPa
Plastic Strain	0

[Downloaded from ijce.iust.ac.ir on 2024-08-14]

Table 6. Torsional moments and rigidity of specimens with and without vulnerable connection

Specimen	State of behavior						Elastic Torsional Rigidity (ITR) (kN-m/rad)
	Torsional moment at relevant state (kN-m)						
	Minor Crack	Visible Crack	Yielding	Hardening	Ultimate	Crack Widening	
UBB	62.42	106.2	138.3	172.2	201.02	183.81	4,087,144.64
NUBB	61	104.92	131.76	168.36	200.08	-	3,166,006.03
NUBB-VC	58.29	86.43	130.65	154.77	192.96	-	1636955.39
SUBB	126.8	293.6	521.3	559.14	624.2	593.1	6433316.17
NSUBB	122.43	279.72	544.32	567	604.96	-	4535680.72
NSUBB-VC	118.56	243.36	505.44	524.88	592.8	-	4112313.22
Specimen Ratios	Ratio of Torsional moment						Ratio of ITR
NUBB/UBB	0.98	0.99	0.95	0.98	1.00	-	0.78
UBB/NUBB-VC	1.07	1.23	1.06	1.11	1.04		2.49
NSUBB/SUBB	0.97	0.95	1.04	1.01	0.97	-	0.71
SUBB/NSUBB-VC	1.07	1.21	1.03	1.07	1.05		1.56
SUBB/UBB	2.03	2.76	3.77	3.25	3.11	3.23	1.58
NSUBB/NUBB	2.01	2.67	4.13	3.37	3.02	-	1.43
NSUBB-VC/NUBB-VC	2.03	2.82	3.87	3.39	3.07	-	2.51

behavior of brick building with vulnerable connection, shown in Figure10-c. In addition, Table 6 provides the torsional moments for specimens with and without vulnerable connections. As it is seen the torsional capacity of the specimen UBB with respect to specimen NUBB-VC is 23% and 6%higher at cracking and yielding states respectively and almost the same at ultimate state. This is most probably due to the fact that the ultimate strength of both buildings is independent to the wall connections as the torsional cracks are start to widen at this stage with the concentration of shear stresses.This difference for elastic torsional rigidity is 149% higher. Therefore the vulnerability of wall-to-wall connection seriously reduces the torsional rigidity rather than the torsional moment. Same results are obtained for the strengthened specimen with the exception of 56% for higher torsional rigidity, which is almost certainly due to the effect of RC overlay. The ratios of numerical models are almost the same as given in Table6.T-θ curves for all experimental and numerical models shown in Figure 10 clearly illustrate the effect of RC overlay used for strengthening of unreinforced masonry buildings and the effect of vulnerability of wall-to-wall connections.

Fig. 11. Vulnerable wall-to-wall connection failed in Bam earthquake, Iran 2000

5. Conclusion

In this paper, experimental and numerical analysis carried out to find the effect of simple strengthening method (reinforced concrete overlay) on nonlinear torsional behavior of single story brick building and verifying the vulnerability of wall-to-wall connections.Based on the results of the present study, the following conclusions can be drawn:

1. Externally reinforced concrete overlay was shown from experiments to be a viable form of torsional strengthening for unreinforced brick buildings.
2. Increases in cracking, yielding and ultimate torsional moments of strengthened specimen was 176%, 277% and 211% respectively compared to the unstrengthenedspecimen.

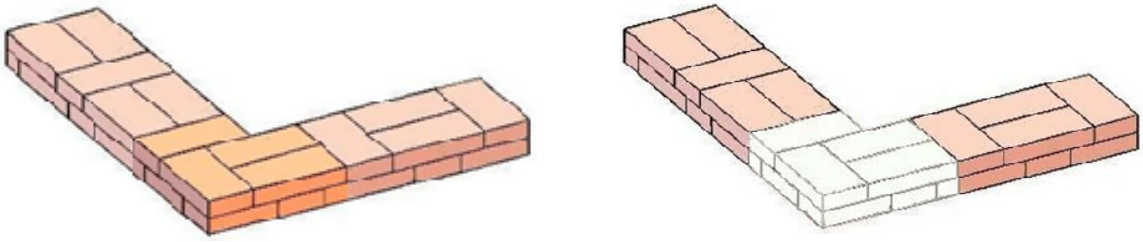

a) Assumed ordinary (Homogeny) Connection

b) Vulnerable connection
(Zero Value for Material Properties)

Fig. 12. Ordinary and vulnerable wall-to-wall connection

[Downloaded from ijce.iust.ac.ir on 2024-08-14]

3. LVDT's measurements provide experimental evidence that the torsional deformation of strengthened specimen is more uniform than that of unstrengthenedspecimen.

4. Good agreement achieved between the results obtained from numerical non-linear finite element modeling and that of experiments interms of torque–twist behavior and crack patterns.

5. The failure mode of strengthened specimen was a combination of diagonal tension and sliding while that of unstrengthened specimen was diagonal tension only. This indicates that the strengthening changes the brittle failure to ductile failure.

6. Vulnerable wall-to-wall connection in brick building reduces the torsional strength at cracking, yielding states and severely the elastic torsional rigidity.

7. Strengthening of vulnerable wall-to-wall connections of brick building without any confining elements (RC vertical ties), significantly increases the torsional strength and elastictorsional rigidity.

The above conclusions are restricted to single story brick buildings under simple torsion. Realistic torsional behavior of asymmetric buildings should be explored in further investigations.

Acknowledgment: Building and Housing Research Center (BHRC) sponsored the experimental investigation of this research under grant No. 1-7174-b. Their funding is gratefully acknowledged. However, opinions expressed in this paper are those of the writers, and do not necessarily represent those of BHRC.The experimental work of this study was conducted in the Structural Laboratory at BHRC. The assistance of all laboratory staff is highly appreciated.

References

[1] ElGawady, M., Lestuzzi, P., and Badoux, M., 2004, A Review of Conventional Seismic Retrofitting Techniques for URM, Proceedings of 13th IB2MC, Amsterdam, the Netherland, Paper No. 89.

[2] Franklin, S., Lynch, J., and Abrams, D.P., December 2001, Performance of Rehabilitated URM Shear Walls: Flexural Behavior of Piers, Mid-America Earthquake Center, Department of Civil Engineering, University of Illinois at Urbana-Champaign, Illinois, the USA.

[3] Karantoni F., Fardis M., 1992, Effectiveness of seismic strengthening techniques for masonry buildings, J. Struc. Eng., ASCE, 118(7), 1884-1902.

[4] Elgawady, M.A., Lestuzzi, P., and Badoux, M., 2006, Retrofitting of Masonry Walls Using Shotcrete, 12th World Conference on Earthquake Engineering, NZSEE,Auckland, New Zealand, and Paper No.45.

[5] Albert, M.L., Cheng, J.J.R., and Elwi, A.E., 1998, Rehabilitation of Unreinforced Masonry Walls with Externally Applied Fiber Reinforced Polymers, Structural Engineering Report, No. 226, Department of Civil and Environmental Engineering, University of Alberta, Edmonton, Canada.

[6] Grillo, V.E., 2003, FRP/Steel Strengthening of Unreinforced Concrete Masonry Piers, M.Sc. Dissertation, Department of Civil Engineering, University of Florida, Florida, the USA.

[7] Abrams, D. P., Lynch, J. M., 2001, Flexural behavior of retrofitted masonry piers, KEERC-MAE Joint Seminar on Risk Mitigation for Regions of Moderate Seismicity, Illinois, USA.

[8] Kahn L. F., 1984, Shotcrete retrofit for unreinforced brick masonry, 8th WCEE, USA, 583-590.

[9] Tomazevic M., 1999, Earthquake resistant design of masonry buildings, Imperial College Press, London, England.

[10] Hutchison D., Yong P., McKenzie G., 1984, Laboratory testing of a variety of strengthening solutions for brick masonry wall panels, 8th WCEE, San Francisco, USA, 575-582.

[11] American Society for Testing and Materials (ASTM), (2000), "Standard test methods for sampling and testing brick and structural clay tile." ASTM C-67-00, Annual book of ASTM standards, Vol. 04.05, West Conshohocken, Pa.

[12] American Society for Testing and Materials (ASTM), (2000), "Standard Test Method for Compressive Strength of Cylindrical Concrete Specimens." ASTM C39/C39M-99, Annual book of ASTM standards, Vol. 04.05, West Conshohocken, Pa.

[13] American Society for Testing and Materials (ASTM), (2000), "Standard Test Method for Splitting Tensile Strength of Cylindrical Concrete Specimens." ASTM C496-96, Annual book of ASTM standards, Vol. 04.05, West Conshohocken, Pa.

[14] American Society for Testing and Materials (ASTM), (2000), "Standard test method for compressive strength of masonry prisms." ASTM C-1314-2000a, Annual book of ASTM standards, Vol. 04.05, West Conshohocken, Pa.

[15] Paulay, T. and Priestley, M. J. N. (1992) "Seismic design of reinforced concrete and masonry buildings." John Wiley & Sons, Inc., New York, NY, USA.

[16] Harris H. G. and Sabnis G. M. (1999) "Structural modeling and experimental techniques." CRC Press, New York, NY, USA.

[17] INBC-Part 8, (2005), "Design and Construction of Masonry Buildings", Iranian National Building Code, Part 8, Ministry of Housing and Urban Development, I.R. Iran.

[18] Lourenco P.B., (1996), Computational strategies for masonry structures, Ph.D. thesis, Delft University of Technology, Delft, The Netherlands.

[19] Luisa Berto, Anna Saetta, Roberto Scotta, Renato Vitaliani. Shear behaviour of masonry panel: Parametric FE analyses. J. International Journal of Solids and Structures 2004; 41:4383-4405.

[20] Lourenco P B , Jan G R. Multisurface interface model for analysis of masonry structures. Journal of Engineering Mechanics 1997; 123(7):660-668.

[21] Massart T.J, Peerlings R.H.J , Geers M.G.D. Mesoscopic modeling of failure and damage-induced anisotropy in brick masonry. European Journal of Mechanics A/Solids 2004; 23:719-735.

[22] Gabor A, Ferrier E, Jacquelin E, Hamelin P. Analysis and modeling of the in-plane shear behavior of hollow brick masonry panels. Construction and Building Materials 2005.

[23] Massart T.J, Peerlings R.H.J , Geers M.G.D, Gottcheiner S. Mesoscopic modeling of failure in brick masonry accounting for three-dimensional effect. Engineering Fracture Mechanics 2005; 72:1238-1253.

[24] IS2800, (2005), "Iranian Code of Practice for Seismic Resistant Design of Buildings, Standard No. 2800", 3rd Edition, Published by BHRC, PN S 253: Tehran, I.R. Iran.

[Downloaded from ijce.iust.ac.ir on 2024-08-14]